https://doi.org/10.1016/j.enconman.2017.02.072

Energy Upcycle in Anaerobic Treatment: Ammonium, Methane, and Carbon Dioxide Reformation through a Hybrid Electrodeionization–Solid Oxide Fuel Cell System

Linji Xu[1,2], Feifei Dong[3], Huichuan Zhuang[1], Wei He[3], Meng Ni [2,3], Shien-Ping Feng[4], Po-Heng Lee[1,2*]

[1]*Department of Civil and Environmental Engineering, The Hong Kong Polytechnic University, Hung Hom, Kowloon, Hong Kong SAR, P. R. China.*
[2]*Research Institute for Sustainable Urban Development, The Hong Kong Polytechnic University, Hung Hom, Kowloon, Hong Kong SAR, P. R. China.*
[3]*Department of Building and Real Estate, The Hong Kong Polytechnic University, Hung Hom, Kowloon, Hong Kong SAR, P. R. China.*
[4]Department of Mechanical Engineering, The University of Hong Kong, Pokfulam, Hong Kong
[*]*Corresponding author: phlee@polyu.edu.hk; phone: +852-2766-6067; fax: +852 2334 6389*

ABSTRACT

To create possibilities for a more sustainable wastewater management, a novel system consisting of electrodeionization (EDI) and solid oxide fuel cells (SOFCs) is proposed in this study. This system is integrated with anaerobic digestion/landfills to capture energy from carbonaceous and nitrogenous pollutants. Both EDI and SOFCs showed good performances. EDI removed 95% and 76% ammonium-nitrogen (NH_4^+-N) from diluted (0.025 M) to concentrated (0.5 M) synthetic ammonium wastewaters, respectively, accompanied by hydrogen production. SOFCs converted the recovered fuels, biogas mixtures of methane and carbon dioxide, to electricity. Under the optimal conditions of EDI (3.0 V applied voltage and 7.5 mm internal electrode distance (IED), and SOFCs (750 °C operating temperature), the system achieved 60% higher net energy output as compared to conventional systems. The estimated energy benefit of this proposed system showed that the net energy balance ratio is enhanced from 1.11 (existing system) to 1.75 (this study) for a local Hong Kong active landfill facility with 10.0 g L^{-1} chemical oxygen demand (COD) and 0.21 M NH_4^+-N. Additionally, an average of 80% inorganic ions (heavy metals and nutrient elements) can be removed from the raw landfill leachate by EDI cell. The results are successful demonstrations of the upgrades of anaerobic processes for energy extraction from wastewater streams.

1 Introduction

Energy extraction from wastewater streams has gained increasing attention to eliminate environmental threats and offset fossil fuel consumption [1-4]. The most readily adaptable approaches are anaerobic treatment, e.g., anaerobic digestion (AD) or landfill, converting wastewater or municipal solid waste into biogas (approximately 60% methane (CH_4)/ 40% carbon dioxide (CO_2) volume/volume [v/v]) and ammonium-rich fermentation broth/leachate (400 mg L^{-1} to 8000 mg L^{-1} NH_4^+-N) [5-8]. Although biogas is well established as a fuel for electricity generation via combined heat and power (CHP) or cogeneration with gas engines [9-11], the electricity conversion efficiency is usually limited to around 30% [12, 13]. Moreover, ammonium-rich wastewater, discharged without proper treatment, brings severe environmental impacts [14-17]. Further improvements and updates are hence necessary and urgent.

Conventionally, NH_4^+-N in fermentation broth/leachate can be removed through adding an alkali to raise the pH level over its pK_a value (9.25) followed by physicochemical methods such as microwave radiation, air stripping (AS), and heating [18-22]. Biological nitrogen removal processes such as nitrification–denitrification, nitrification shortcut, and anaerobic ammonium oxidation have also been applied [21, 23]. These approaches require expensive chemicals and consume intensive energy [18-22]. Ammonia (NH_3) can be used as an alternative fuel to hydrogen (H_2) [24]. Upon decomposition, NH_3 produces two harmless gases (nitrogen

63 [N_2] and H_2), and simultaneously releases 320 kJ mol^{-1} chemical energy. Theoretically,
64 this process produces approximately 10% more energy than H_2 oxidation (285 kJ mol^{-1}) [25-27]. Since NH_3 has special properties (incombustibility, incomplete
66 decomposition, toxicity, and solubility), its energy potential has not been highly
67 recognized yet [28, 29]. For wastewater in which NH_3 exists in the form of NH_4^+ ion,
68 the low conversion efficiency from NH_4^+ ion to NH_3 gas, high cost, and NO_x emissions
69 also reduce the motivation to explore its energy potential [30].
70
71 SOFC is a promising energy conversion technology. It is capable of electrochemical
72 converting a variety of gas fuels (H_2, NH_3, CH_4 and other hydrocarbon compounds)
73 into electricity. Also, it has an energy conversion efficiency as high as 50% [31, 32].
74 The upper right-hand panel of Fig. 1 illustrates the power generation mechanism of
75 SOFCs. (I) When CH_4 is fuel, it reforms with H_2O or CO_2 and produces H_2 and CO at
76 the anode under the high-temperature condition. (II) These reformed gases react
77 with oxygen ions (O^{2-}) and produce CO_2 and H_2O, and release electrons (e^-). (III) The
78 released electrons flow through the external circuit and they are collected by the
79 current collector to produce electrical power. (IV) Once electrons reach the cathode,
80 they are accepted by O_2 molecule and O^{2-} ions are produced again. In this cycle, O_2
81 and gas fuels are consumed for electricity generation.
82
83 SOFCs have some advantages for gas production from wastewater. As SOFCs generate
84 electrical power in a straightforward way through electrochemical reactions and does

not go through thermodynamic cycles, its power generation efficiency is not limited by the Carnot efficiency [33]. Although carbon deposition is an issue for SOFCs fed with pure CH_4, this issue might be solved for biogas because its reformation with H_2O or CO_2 generates gases instead of solid carbon [34-36]. As such, biogas is potentially a good fuel for power generation systems using SOFCs [37]. Another potential fuel for SOFCs is NH_3 gas. When NH_3 is fed into SOFCs, it is thermally decomposed into N_2 and H_2. Subsequently, H_2 goes through the same reaction process with other gas fuels [38]. Studies have found that carbon deposition can be prevented by adding NH_3 to CH_4 as well [31, 39]. Therefore, this novel system of integrating SOFCs with AD and landfill facilities is proposed to convert NH_3 and biogas into electrical power for simultaneous pollution control.

The main issue with this system is that the aqueous NH_4^+ in fermentation broth/leachate requires an additional conversion step to NH_3 gas so as to be fed into SOFC. As aforementioned, the existing approaches for NH_3 gas recovery are both uneconomic and environmentally unfriendly[40-42]. Hence, advanced technologies are required. EDI is an attractive technology because it has an excellent selectivity for target ion. Ion migration is driven by electric potential gradients rather than by physical pressure [43, 44]. As shown in the bottom right panel of Fig. 1, directional movement leads to accumulation of target ions such that the concentrated ions can be harvested with low energy consumption. As Mondor et al. reported, EDI has been used to produce fertilizers from swine manure with 1.0 kWh kg^{-1} NH_3 energy input,

saving 1.8 kWh kg^{-1} NH_3 compared to 2.8 kWh kg^{-1} NH_3 required for AS [45]. Moreover, the applied voltage leads to water splitting. The generated H_2 in the cathode is an additional fuel for SOFCs [46], while hydroxide (OH^-) creates an alkaline condition and promotes the transformation from NH_4^+ into NH_3. Consequently, the dosage of alkaline can be reduced, and more energy can be captured.

Compared to other energy conversion processes, this proposed system could yield theoretical energy output. For example, Scherson et al. recently reported that coupled aerobic–anoxic nitrous decomposition operation (CANDO) for NH_4^+ wastewater treatment could yield a more powerful oxidant (N_2O) than O_2 because it released an additional energy of 82 kJ mol^{-1} from N_2O to N_2 (Eq. 1) [23]. One mole of CH_4 combusted with 4 moles of N_2O releases -1219 kJ mol^{-1} (Eq. 2), approximately 30% more stoichiometric energy than combustion with 2 moles of O_2 (Eq. 3)

$$N_2O_{(g)} \rightarrow 0.5O_{2(g)} + N_{2(g)} \qquad \Delta H_R^0 = -82 \text{ kJ mol}^{-1} \quad (1)$$

$$CH_{4(g)} + 4N_2O_{(g)} \rightarrow CO_{2(g)} + 2H_2O_{(l)} + 4N_{2(g)} \qquad \Delta H_R^0 = -1219 \text{ kJ mol}^{-1} \quad (2)$$

$$CH_{4(g)} + 2O_{2(g)} \rightarrow CO_{2(g)} + 2H_2O_{(l)} \qquad \Delta H_R^0 = -890 \text{ kJ mol}^{-1} \quad (3)$$

In SOFCs, NH_3 releases nearly four times more energy than same stoichiometric N_2O dissociation (Eq. 1 and Eq. 4). Theoretically, if both CH4 and NH3 serve as fuels, -2125 kJ mol^{-1} is released (Eq. 5), which is 906 kJ mol^{-1} more energy output than N_2O as an oxidant (Eq.2). This energy potential implies that NH_3 is a promising additional fuel. Additionally, the H2 generated in EDI releases an extra 285 kJ mol^{-1}, if water dialysis occurs (Eq. (6)).

$$NH_{3(g)}+0.75O_2 \rightarrow 0.5N_{2(g)}+1.5H_2O_{(l)} \quad \Delta H_R^0 = -320 \text{ kJ mol}^{-1} \quad (4)$$

$$CH_{4(g)}+4NH_{3(g)}+5O_{2(g)} \rightarrow CO_{2(g)}+2N_{2(g)}+8H_2O_{(l)} \quad \Delta H_R^0 = -2125 \text{ kJ mol}^{-1} \quad (5)$$

$$H_{2(g)}+0.5O_{2(g)} \rightarrow H_2O_{(l)} \quad \Delta H_R^0 = -285 \text{ kJ mol}^{-1} \quad (6)$$

Accordingly, the novel hybrid AD-EDI–SOFC system illustrated in Fig. 1 has potential to capture more energy from biogas and fermentation broth/leachate. Hopefully this system provides more sustainable wastewater management for the anaerobic treatment and landfill processes.

2 Materials and Methods

2.1 EDI Stack

A two-channel EDI reactor (effective volume of each channel 20 mL) was constructed. The anode and cathode (the bottom right down panel of Fig. 1) were made of two square Perspex frames with same internal dimensions (6 cm × 6 cm × 0.5 cm), separated by 1 mm-thickness cation exchange membrane (IONSEP® AM-C, Hangzhou Iontech Environmental Technology CO., Ltd, China). The anode electrode is titanium (Ti) coating platinum (Pt) (4 cm × 4 cm × 1 mm) (Shenzhen 3N Industrial Equipment CO., Ltd., China), and the cathode is Ti coating iridium ruthenium molybdenum (Ir-MMO) with same dimensions. After fixing anode and cathode, EDI stack was sealed by a 2 mm-thick silica sheet and locked by screws. The anode was fed with synthetic wastewater containing 0.0125 to 0.25 M ammonium sulfate, $(NH_4)_2SO_4$. The cathode was filled with sodium sulfate, (Na_2SO_4) with same

concentrations as the supporting electrolyte. All batch of tests were carried out at room temperature (25 ± 2 °C). Each set of experiments was set at a series of applied voltages (0.5V to 8.0 V) with 2.0 h per cycle. The variations of the real-time current and voltage were recorded by a Keithley 2700 multimeter (Tektronix, Inc., USA). The electrochemical behaviors of electrodes (Cycle voltammetry, CV) were analyzed using an electrochemical working station (CorrWare®, Scribner Associates Inc., USA). After applied voltage optimization, IED was set at 7.5, 15.0, 30.0, 60, and 80.0 mm per 2.0 h per cycle under the optimal applied voltage.

Based on the results of laboratory-scale EDI tests, the semi-continuous tests using a raw landfill leachate as feed were conducted using a three-channel EDI reactor (Fig. S1). The leachate was obtained from the West New Territories Landfill (Nim Wan, Tuen Mun, Hong Kong). The leachate was fed into the middle channel at an influent rate of 2 mL min^{-1}. The anode and the cathode channels were filled with 0.005 M hydrogen sulfate (H_2SO_4) and Na_2SO_4, respectively. The generated gases were collected using gas-sampling bags.

2.2 Button-type Solid Oxide Fuel Cells

Three-layer button SOFC reactors were constructed to be electricity generation units. Single cell with an anode-supported, thin-film dual-layer electrolyte configuration was prepared via a tape casting process, spray deposition and subsequent high-temperature sintering. The diameter was 1.0 cm and the active area was 0.48 cm^2. The

fuel cells tested in this study consisted of NiO+$(ZrO_2)_{0.92}(Y_2O_3)_{0.08}$ (YSZ, NiO:YSZ = 6:4 by weight) anode, YSZ electrolyte, $Sm_{0.2}Ce_{0.8}O_{1.9}$ (SDC) interlayer and $Ba_{0.5}Sr_{0.5}Co_{0.8}Fe_{0.2}O_{3-\delta}$ (BSCF) cathode. BSCF has been recently used as a benchmark cathode material for SOFC, due to its better electrochemical activity over that of LSM and LSCF [47]. BSCF and SDC powders were synthesized using a combined EDTA-citrate complexing sol-gel process [48]. NiO and YSZ are commercial products obtained from Chengdu Shudu Nano-Science Co., Ltd., and Tosoh, respectively. The details for preparing anode substrates NiO+YSZ through the tape casting process are available in the literature [49].

The fabrication of electrode and electrolyte includes several steps. First, the YSZ|SDC double electrolyte layers were constructed using a wet powder spraying technique. The YSZ suspension was sprayed onto the anode substrate using a spraying gun followed by calcination at 1400 °C for 5 h, and the procedure was subsequently repeated for the SDC suspension (buffering layer) deposited onto the thick YSZ surface [50]. The resultant three-layered pellets were then calcined at 1350 °C for 5 h in air. Finally, BSCF slurry was sprayed onto the surface of the SDC interlayer and fired at 1000 °C for 2 h in air to function as the cathode layer.

The current–voltage curves of the button fuel cells operated at 550–750 °C were obtained using a Keithley 2420 source meter (Tektronix, Inc., USA) based on a four-probe configuration. During the test, H_2, NH_3–H_2, CH_4–CO_2 gas mixtures and a biogas

generated from a laboratory-scale digester were fed into the anode chamber at a flow rate of 100 ml min^{-1} with ambient air serving as the oxidant gas in the cathode chamber. Biogas with a composition of 68% CH_4 and 32% CO_2 (v/v) was obtained in the laboratory from a semi-continuous AD reactor fed with local sewage sludge (S1).

2.3 Chemical Analysis

NH_4^+-N was measured using the Berthelot method, and NH_3 was absorbed by 1 M H_2SO_4, then detected with the same approach. Nitrite, nitrate, phosphate, and sulfate were measured according to standard methods [51]. Total nitrogen was analyzed with 720 °C catalytic thermal decomposition/chemiluminescence methods using TOC-L analyzers (TOC-LCSH/CPH, Shimadzu). H_2 was determined by gas chromatography (Agilent 4890D; J&W Scientific, USA) using a HP-MoleSieve column (30 m × 0.53 mm × 50 m) [52]; Helium gas served as the carrier gas and was injected at a rate of 6 mL min^{-1}. The temperatures of the injection port, column, and the thermal conductivity detector were 200 °C, 35 °C, and 200 °C, respectively. Samples (200 µL) were injected by micro syringes (Shanghai Anting Scientific., China). The determination of heavy-metal ions was conducted using an Agilent 7500cx ICP-MS (Agilent Technologies, Santa Clara, CA, USA) [53]. The detailed measurements and analyses are available in the supporting material (S1 and Eq. S1 and Eq. S2).

2.4 Calculation

Energy balance ratio (EBR)

The EBR is the energy input to output as expressed by Eq. 7 to evaluate the efficiency of the EDI–SOFC system.

$$EBR = \frac{W_{out} \times r}{W_{in}} \quad (7)$$

where W_{out} is the enthalpy of CH_4, NH_3 and H_2, respectively; r is the electricity conversion efficiency of SOFCs; and W_{in} is the energy consumption.

W_{in} is calculated as follows:

$$W_{in} = \sum(\Delta W) = \sum(I \times \varphi_{ap} \times dt) \quad (8)$$

$$W_{in} = Q \times \varphi_{ap} \quad (9)$$

$$Q = I \times t = \int i \times dt \quad (10)$$

where φ_{ap} is the applied voltage; Q is the electric quantity; $W_{out} = m_j \times \Delta H$, m_j is the mass of fuels, and ΔH is enthalpy.

3 Results

3.1 Ammonium Deionization

Optimizations of applied voltage, internal electrode distance and NH_4^+ concentration in the EDI were investigated through adjustments of applied voltage (0.5–8.0 V), IED (7.5–80 mm), and influent NH_4^+ concentrations (0.025–0.5 M) (Fig. 2 and Table 1). The deionization efficiency of NH_3 increases linearly with an increase in applied voltage, and reaches a maximum value of 80% at 8.0 V. The corresponding EBR, based on the recoveries of NH_3 and H_2, are 1.67 and 0.86 at 3.0 V and 8.0 V, respectively, when the IED is 15 mm (Fig. 2a), indicating that 3.0 V is the optimal

voltage. This result is lower than the voltage of 17.5 V reported previously [54].

At this applied voltage, as the IED narrowed from 15 mm to 7.5 mm, the deionization efficiencies of NH_3 and EBR reciprocally increases from 64.8% and 1.67 to 84.8% and 1.99, respectively. However, when the IED is expanded to 60 mm the deionization efficiencies of NH_3 and EBR decrease to 12% and 1.09, respectively, (Fig. 2b). This variation of NH_4^+ deionization efficiency signifies that the influence of the internal electrode length is much more important than that of the applied voltage, which can be verified by Stock's model [55, 56]. Regarding the effects of ions, the drift velocity has a positive correlation with applied voltage but a negative relationship with the electrode distance. More details are available in the supporting information (S2, Eq. S3, and Figs. S2a and S2b). The deionization rate at the optimal applied voltage and IED increases to 80 mM d^{-1} within 0.5 h but drops to 20 mM d^{-1} at 2.0 h, indicating that deionization efficiency does not increase with extended operating time (Fig. S2c). This effect is likely to be related to Donnan equilibrium, where ion migration comes to a stop as the concentration gradient narrows [57, 58].

3.2 Ammonium Dissociation

An interesting observation was the formation of N_2 at the cathode instead of the commonly-reported anode. In this regard, we investigated the mass balance of total nitrogen and electrode behaviors (Fig. 3). The nitrogen compounds (NH_4^+, NH_3, and N_2) were detected while the other compounds were not detected due to below

detection levels of 0.2 ng L^{-1}. As shown in Fig 3a, approximately 60%, 30%, and 10% of nitrogen exist in the forms of NH_4^+, NH_3, and N_2 for synthetic wastewater. Fig. 3a also shows the nitrogen compounds of raw landfill leachate. 87.5%, 1.7%, and 0.38% of nitrogen exist in the forms of NH_4^+, NH_3, and N_2, respectively. The conversion efficiency of NH_4^+ to NH_3 for synthetic wastewater is higher than that for raw landfill leachate, which is attributed to the complex constitution of the raw landfill leachate. In addition, since ions differ in their properties of size, valence, diffusion coefficient, and conductivity, they exhibit different migration kinetics. For example, the mobility order of H^+, K^+, NH_4^+ and Na^+ is $H^+ > K^+ > Na^+ > NH_4^+$ [59].

N_2 formation may be related to NH_3 reduction. To prove this hypothesis, we carried out CV tests at a scanning rate of 0.5 to 10 mV s^{-1} in the range of 0–1.5 V using Ag/AgCl as the reference electrode (Fig. 3b). Only a reduction peak at around 0.3 V is observed on each CV curve, indicating the possible electrochemical dissociation of NH_4^+. However, to date, this phenomenon has not received much scientific attention. Only a few references describe this phenomenon. As reported by Simons et al., the mechanism of NH_4^+ dissociation is a two-step process (Eq. 12 and Eq. 13), and its main products are H_2 and NH_3, accompanied by a small amount of N_2 [60]. The second step is strictly dependent on the concentration of aqueous NH_3. It is known that the concentration of $NH_{3(aq)}$ is determined by the kinetics of the following equilibrium reaction (Eq. 14).

$$NH_4^+ \leftrightarrow NH_3 + 0.5H_2 \qquad (12)$$

283 $$NH_3 \leftrightarrow 0.5N_2 + 1.5H_2 \quad (13)$$

284 $$NH_4^+ + OH^- \leftrightarrow NH_3 \cdot H_2O \leftrightarrow NH_3 + H_2O \quad (14)$$

285 The increasing NH_4^+ concentration and OH^- ion generation promote the shift in
286 equilibrium favoring NH_3 production. The reduction of NH_3 to N_2 and H_2 might occur,
287 when $NH_{3(aq)}$ reaches a certain concentration. NH_4^+ dissociation through the EDI
288 favorably contributes to NH_3 and H_2 yields.

289

290 **3.3 SOFC Performances**

291 3.3.1 Polarization curves of ammonia-hydrogen as fuel

292 To maximize the energy output, the performance of SOFCs was studied with pure H_2
293 at 100.0 mL min^{-1}, operating temperatures of 550–750 °C. The polarization curves
294 show that an open circuit voltage value (OCV) of 1.134 V is obtained at 750 °C (Fig. S3).
295 This operation approaches closest to the Nernst potential of 1.23 V, indicating solid
296 electrolytes and gas-tight sealing [61].

297

298 At 750 °C with H_2 from 20% to 60% by volume (v/v) of NH_3 in the NH_3–H_2 stream, SOFC
299 achieves an OCV of 1.056–1.085 V, slightly lower than that obtained from pure H_2 (Fig.
300 4a). This trend caused by lower H_2 partial pressure in NH_3–H_2 is consistent with the
301 results of the theoretical simulation performed by Meng et al. [62]. The peak power
302 density declines from 1194 mW cm^{-2} at 20% NH_3 to 1018 mW cm^{-2} at 60% NH_3. This
303 phenomenon might be related to insufficient H_2 supply from NH_3 decomposition.
304 Along with the increase in NH_3 concentration, the incomplete decomposition of NH_3

easily occurs, as reported by Denver [63]. In addition, ammonia decomposition is an endothermic process. High concentration NH_3 absorbs too much thermal energy so that the local temperature declines, thereby, the electrochemical reaction rate decreases [64]. The above results can be further explained by the mechanism of NH_3 decomposition (S3 and Eq. S4 to Eq. S6). NO_x were not detected in the off-gas, as expected from reported findings [65, 66].

3.3.2 Polarization curves of methane-carbon dioxide and biogas

With 20%, 40%, 60%, and 80% (v/v) CH_4 in CH_4–CO_2, an increasing trend of OCV value (from ~1 V to ~1.17 V) with an increase of CH_4 was obtained. The slight drop of OCV at 80% CH_4 may be ascribed to the effect of experimental error. Nevertheless, this increasing trend of OCV value (~1 V to ~1.17 V) approaches the theoretical value, indicating a dense electrolyte and decent sealing of SOFC during the testing. For the CH_4–CO_2 mixture in the stability test, apparent carbon deposition was not observed. This result may be related to CH_4 reformation that has been reported elsewhere [67-69]. The mechanism of methane reformation is discussed in the supporting material (S3 and Eq. S7 to Eq. S9). Using biogas (about 70% CH_4) produced from our laboratory-scale AD reactor as the fuel, about 900 mW cm^{-2} peak power density is obtained (Fig. 4c), which is close to the results of the 60% CH_4 and 40% CO_2 mixture. SOFC has been estimated to obtain over 50% energy conversion efficiency, and even close to 80% for CHP applications [70, 71]. From our experimental results of NH_3-H_2, CH_4-CO_2, it is believed that EDI-SOFC is feasible for power generation from biogas and extracted

NH_3-N from fermentation broth/leachate.

3.4 Energy Balance Evaluation of the EDI–SOFC System

The energy balance of EDI-SOFC was investigated for various NH_4^+-N contents (0.025 to 0.5 M) under the optimal conditions obtained previously. EBR value varies with the increase in NH_4^+-N content in synthetic wastewater (Table 1). When the influent NH_4^+-N content is lower than 0.1 M, the EBR is below 1.0, indicating a need for external energy input. As NH_4^+-N increases to 0.25 M, the EBR approaches 1.20, demonstrating 20% of net energy output. An optimal EBR of 1.20 is achieved at 0.25 M of NH_4^+-N. Collectively, it is observed that EBR value increases as NH_4^+-N increases from 0.025 to 0.25 M and decreases once NH_4^+-N reaches 0.50 M. When NH_4^+-N increases from 0.025 M to 0.1 M, due to the changes of conductivity, the current increases. As a result, both energy input and H_2 and NH_3 recovery increase. However, the chemical energy potential of recovered NH_3 and H_2 is not significantly enhanced, and thus its energy input is higher than the energy output. As NH_4^+-N further increases over 0.25 M, the chemical energy potential of recovered NH_3 and H_2 compensates for the energy input. However, the energy input increases significantly at 0.5 M NH_4^+-N, probably due to the increase of current and electric resistances. Taken together, the EDI–SOFC system is most economically feasible for medium to high NH_4^+-N containing waste streams.

To examine the commercial application of this system, the energy potential was estimated using a local raw landfill leachate in Hong Kong. Table S1 summarizes the characteristics of raw landfill leachate. It contains high NH_4^+-N concentration (0.21 M).

As shown in Table 1, 98% of NH_4^+ is removed via the semi-continues EDI stack. The theoretical calculation shows that the EBR approaches 1.76. These results signify that the EDI–SOFC system has an economic strategy for sustainable landfill leachate management.

Table 2 summarizes the potential benefits of the EDI–SOFC system considering oxygen demand, sludge production, and EBR. Compared to conventional nitrification–denitrification [72], nitrification–anammox [73], and CANDO [74]. The EDI has 18.7–50% less sludge yield, no oxygen demand, and 55.9–80.5% less energy consumption despite requiring an energy consumption of 2.32 kWh kg^{-1}-NH_3. Moreover, the Hong Kong West New Territories Landfill was studied to evaluate the integration of the EDI–SOFC system fully. The plant's capacity, biogas yield, and raw leachate properties and its techno-economic evaluation are summarized in Table S1, Fig. 5 and Table S2. The AS-CHP and EDI-SOFC system integrated with the existing plant generates 3.46×10^5 and 4.02×10^5 MWh per year. Regarding the energy inputs, AS-CHP requires 3.29×10^5 MWh per year for NH_3 treatment, while the EDI-SOFC generates 1.0×10^5 MWh per year for NH_3 recovery. Consequently, the EBR can be increased from 1.11 and 1.75, if EDI-SOFC replaces AS-CHP. This result indicates that the EDI–SOFC system can yield about 60% more electricity than the existing system. Additionally, there is 4.04×10^5 MWh energy that goes uncaptured per year. With the incorporation of the EDI-SOFC system, it is believed that more energy can be harvested from landfills.

3.5 Other Inorganic Ion Removal

Aside from NH_4^+ ion, landfill leachate also contains a significant portion of other inorganic ions. Some of them (K^+, Ca^{2+}, Na^+, NO_3^-, PO_4^{3-}, etc.) can be used as fertilizers. Others (Cl^-, Zn^{2+}, Cu^{2+}, Pb^+, Cr^{3+}, etc.) must be removed prior to leachate discharge. Our results show that the conductivity and salinity of the landfill leachate decrease from 88.2 mS cm^{-1} and 7.85% to 2.26 mS cm^{-1} and 0.1%, respectively. EDI has over 80% removal efficacy of cations and high kinetic deionization in K^+, NO_3^-, and PO_4^{3-} (Table 3, Fig. 6, and Fig. S4). Additionally, most of the detected metal ions have larger mobility over NH_4^+ (Fig. 6) due to their smaller ion radii and larger valences [75], suggesting that further separation needs to be considered.

4 Discussion

4.1 Increasing Selective Transfer of Ammonium

Under direct current conditions, the flux of ions in an EDI stack is determined by diffusion and electromigration as described by the Nernst−Planck equation [76]. The concentration-driven process is dependent on the diffusion coefficients of the ions in the solution and the membrane. And electromigration is related to the valence, concentration, and diffusion coefficient, as well as the strength of the electrical field [22, 77]. The positive correlation between NH_4^+ drift velocity and the applied voltage is shown in Fig. S2a. Theoretically, the drift velocity of NH_4^+ can be increased through applying higher voltage. However, this resulted in an opposite effect on the current efficiency of NH_4^+ migration (Table S3). These results indicate that optimal NH_4^+-N

393 deionization can be accomplished at a reasonable range of applied voltage, increasing
394 NH_4^+-N loading and increasing anode flow [22, 78].
395
396 **4.2 Creating a Self-Extracting and Purifying Process for Ammonia**
397
398 Electricity generation of SOFC is associated with NH4 deionization efficiency. Although
399 the EDI batch tests obtain a 30% extraction efficiency, around 60% NH_4^+-N still persist
400 in the liquid phase (Fig. 3a). Increasing NH3 extraction efficiency can be completed in
401 EDI where the alkaline condition (pH > 12) can promote NH_3 evolution. When coupled
402 to AD or landfills, biogas can be served as a stripping gas for NH_3 and H_2 collection.
403 Also, biogas usually contains small amounts of noxious H_2S gas. When biogas flows
404 into the cathode, H_2S is absorbed by OH^-, and thus it is desulfurized to a harmless
405 compound. Finally, biogas, NH_3 and H_2 can be harvested together using only one
406 collector. In this manner, biogas, NH_3 and H_2 production from AD/landfills can be
407 collected without the need for AS and at reduced chemical dosage, lowering the
408 operation cost [79]. Even though the experimental tests have not yet been conducted,
409 this concept is an impetus for us to move forward towards capturing more sustainable
410 energy from wastewater streams through AD/landfill coupled EDI–SOFC system.
411 **5 Conclusions**
412 This study successfully demonstrated the upgrades of anaerobic processes for energy
413 potential extraction from both carbonaceous and nitrogenous pollutants in the EDI-
414 SOFC system. EDI removed 95% and 76% nitrogen from diluted (0.025 M) concentrated

(0.5 M) synthetic NH4 wastewaters, respectively. SOFCs displayed its adaptability with NH_3, H_2, and biogas. The case study of the landfill plant demonstrates that energy benefit is upgraded from 1.11 (existing system) to 1.75 (this study) with this EDI-SOFC system. Additionally, an average of 80% inorganic ions (heavy metals and nutrient elements) was removed from raw landfill leachate by EDI stack.

Acknowledgments

The authors wish to acknowledge financial support from the Blue-Sky Scheme Fund of the Research Institute for Sustainable Urban Development, the Hong Kong Polytechnic University (1-ZVBF) and the Early Career Scheme (ECS) Fund (539213) and Collaborative Research Fund (C7044-14G) of the Research Grants Council (RGC).

Graphic for Manuscript

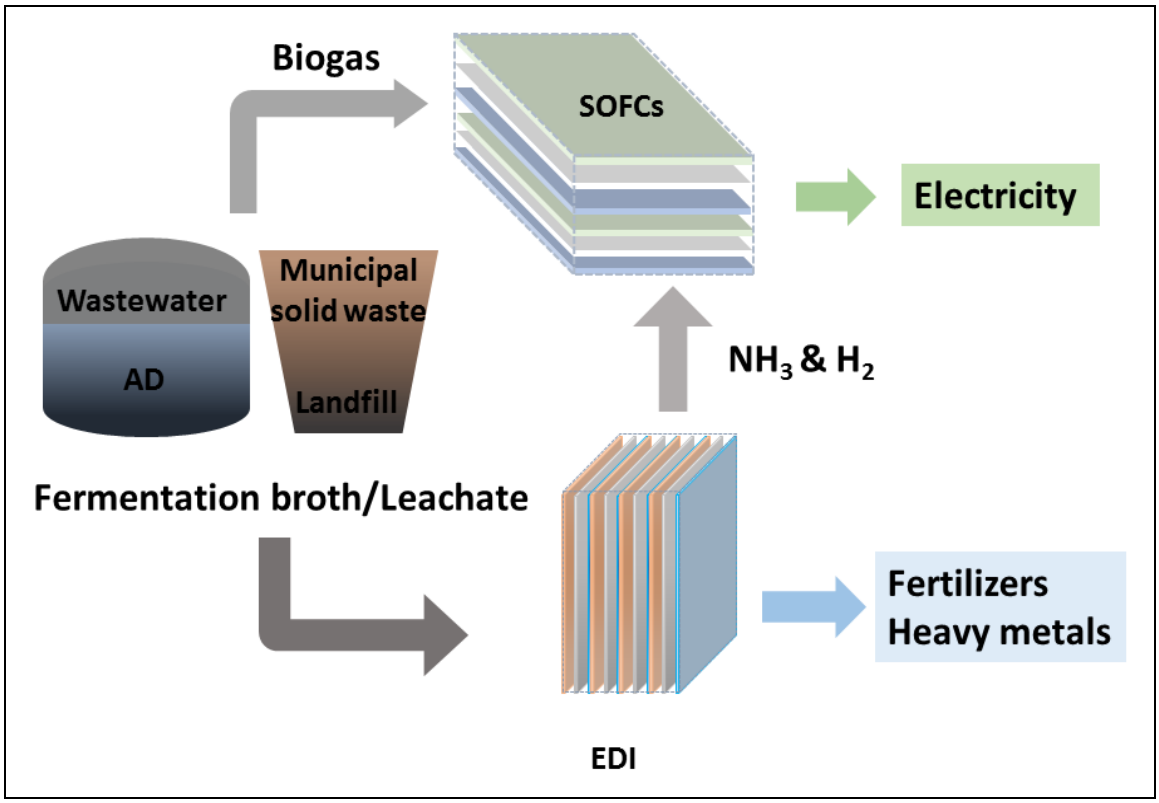

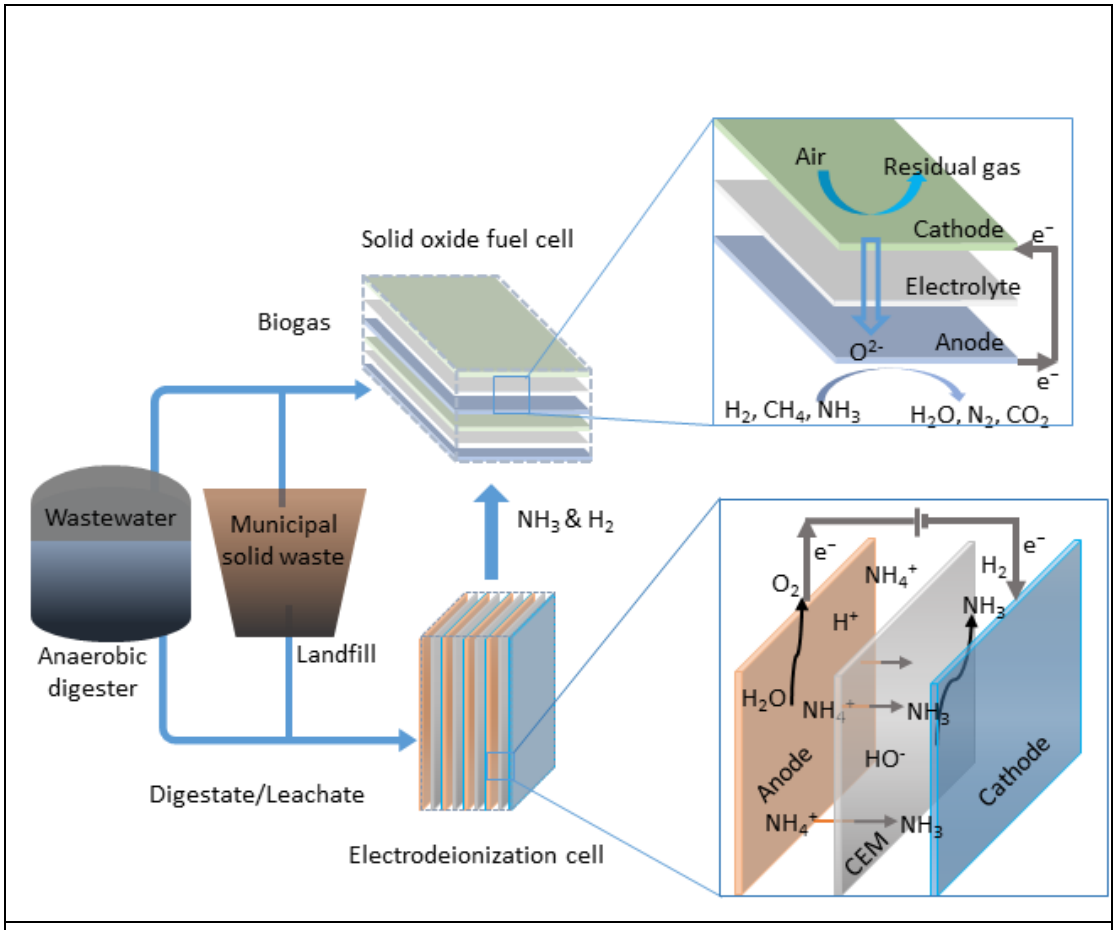

Fig. 1 - Schematic diagram of the EDI–SOFC system integrated with anaerobic treatment

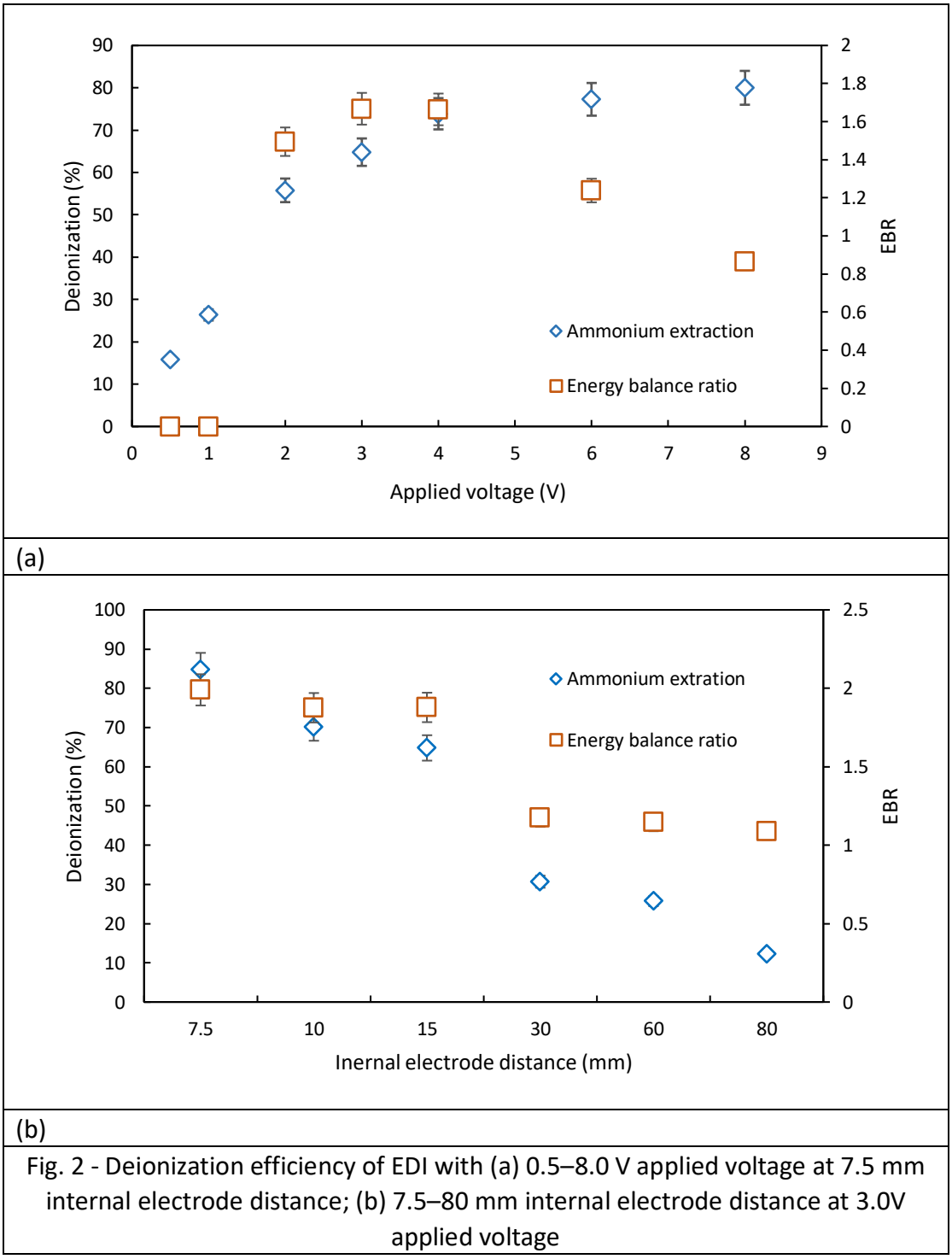

Fig. 2 - Deionization efficiency of EDI with (a) 0.5–8.0 V applied voltage at 7.5 mm internal electrode distance; (b) 7.5–80 mm internal electrode distance at 3.0V applied voltage

455
456
457

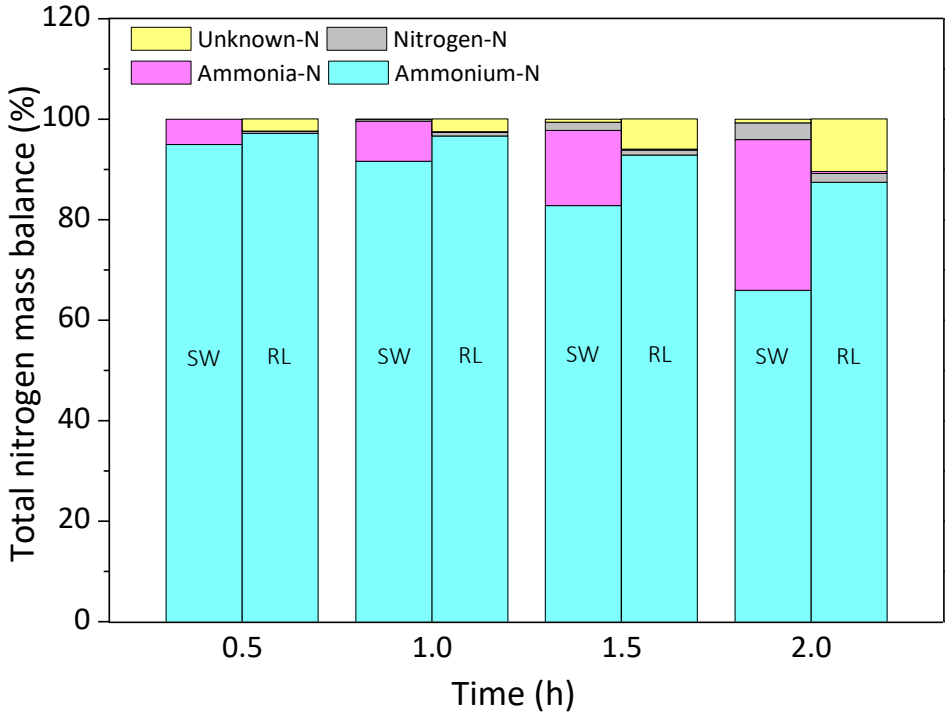

(a)

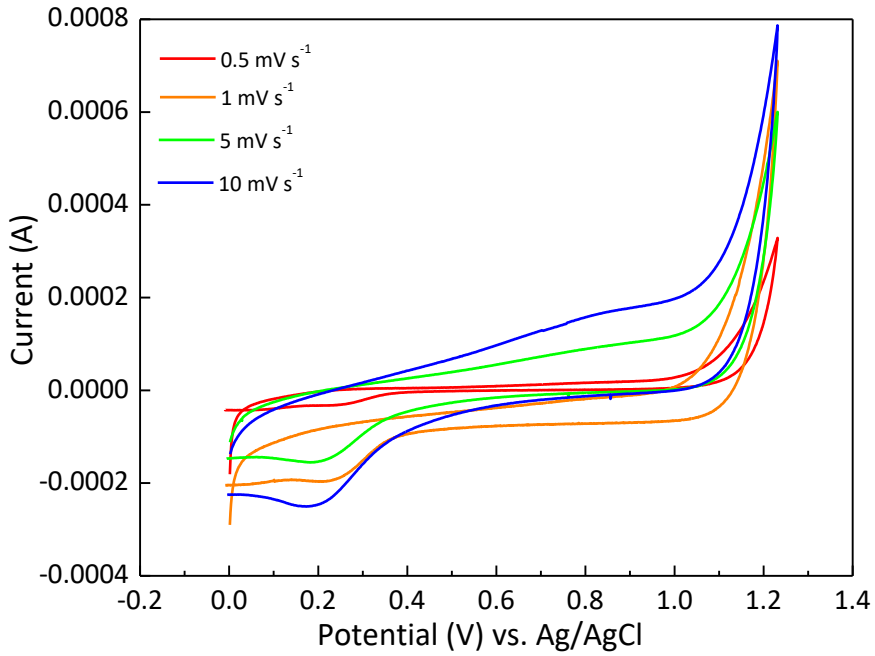

(b)

Fig. 3 (a) Total nitrogen mass balance in terms of ammonium, ammonia, and other nitrogen compounds of synthetic wastewater (SW) and raw landfill leachate (RL); (b) CV curves of EDI at 0–1.23 V vs. Ag/AgCl under 0.5–10 mV s^{-1} for the anolyte

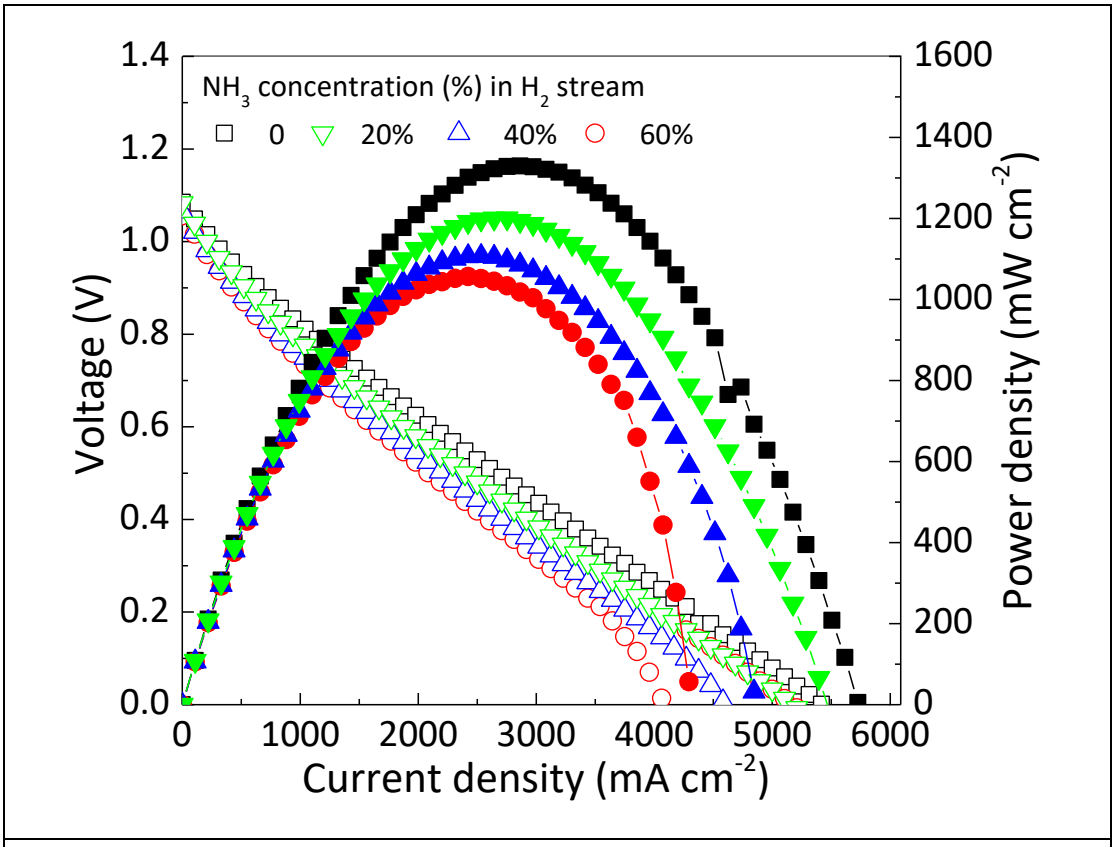
NH3 concentration (%) in H2 stream
0
20%
40%
60%
Voltage (V)
Power density (mW cm-2)
Current density (mA cm-2)
0.0
0.2
0.4
0.6
0.8
1.0
1.2
1.4
0
200
400
600
800
1000
1200
1400
1600
0
1000
2000
3000
4000
5000
6000

(a)

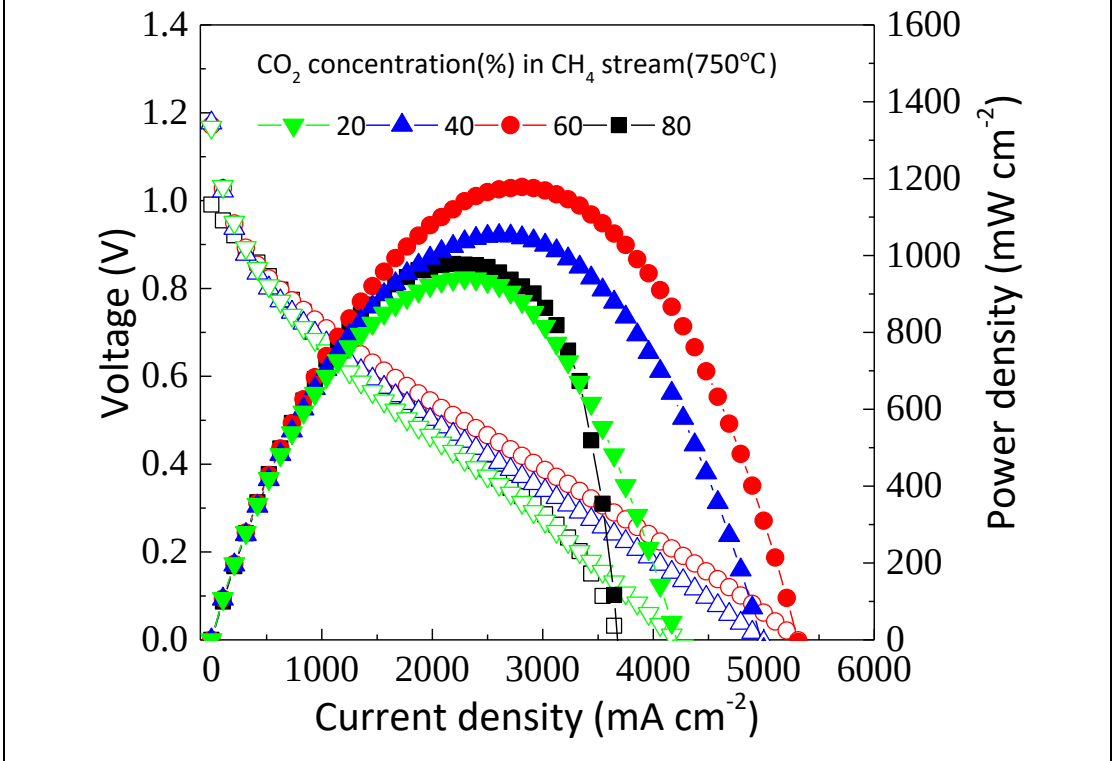
CO2 concentration(%) in CH4 stream(750°C)
20
40
60
80
Voltage (V)
Power density (mW cm-2)
Current density (mA cm-2)
0.0
0.2
0.4
0.6
0.8
1.0
1.2
1.4
0
200
400
600
800
1000
1200
1400
1600
0
1000
2000
3000
4000
5000
6000

(b)

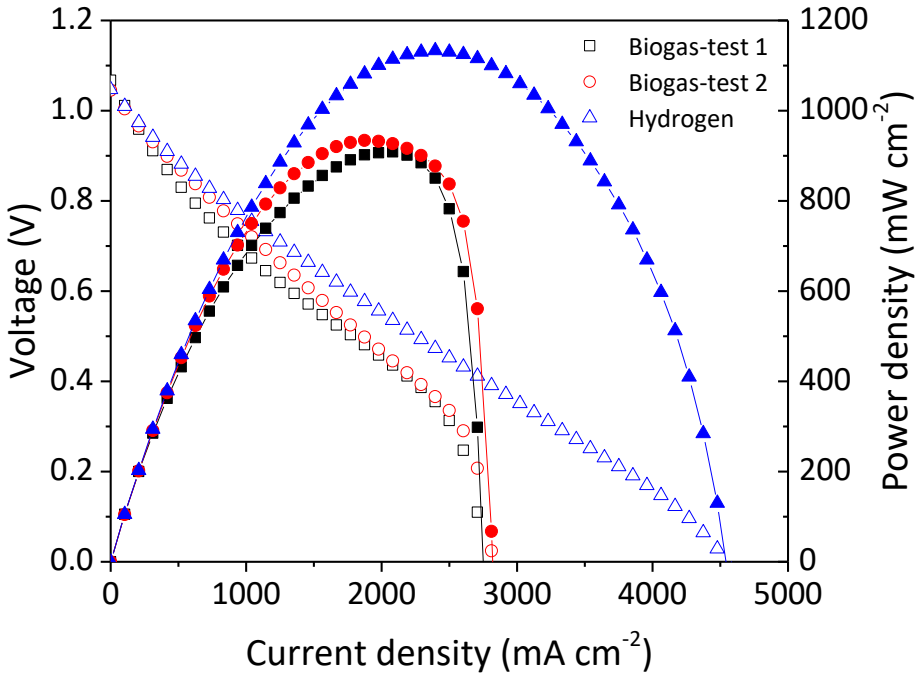

(c)

Fig. 4 V-I and P-I polarization curves of SOFC fed with (a) 0–60% NH_3 in H_2–NH_3 mixture at 750 °C; (b) 20–80% CH_4 in CO_2–CH_4 mixture at 750 °C; (c) Biogas with a mixture of 68% CH_4 and 32% CO_2 (v/v) from a laboratory-scale AD reactor at 750 °C

458
459
460
461
462

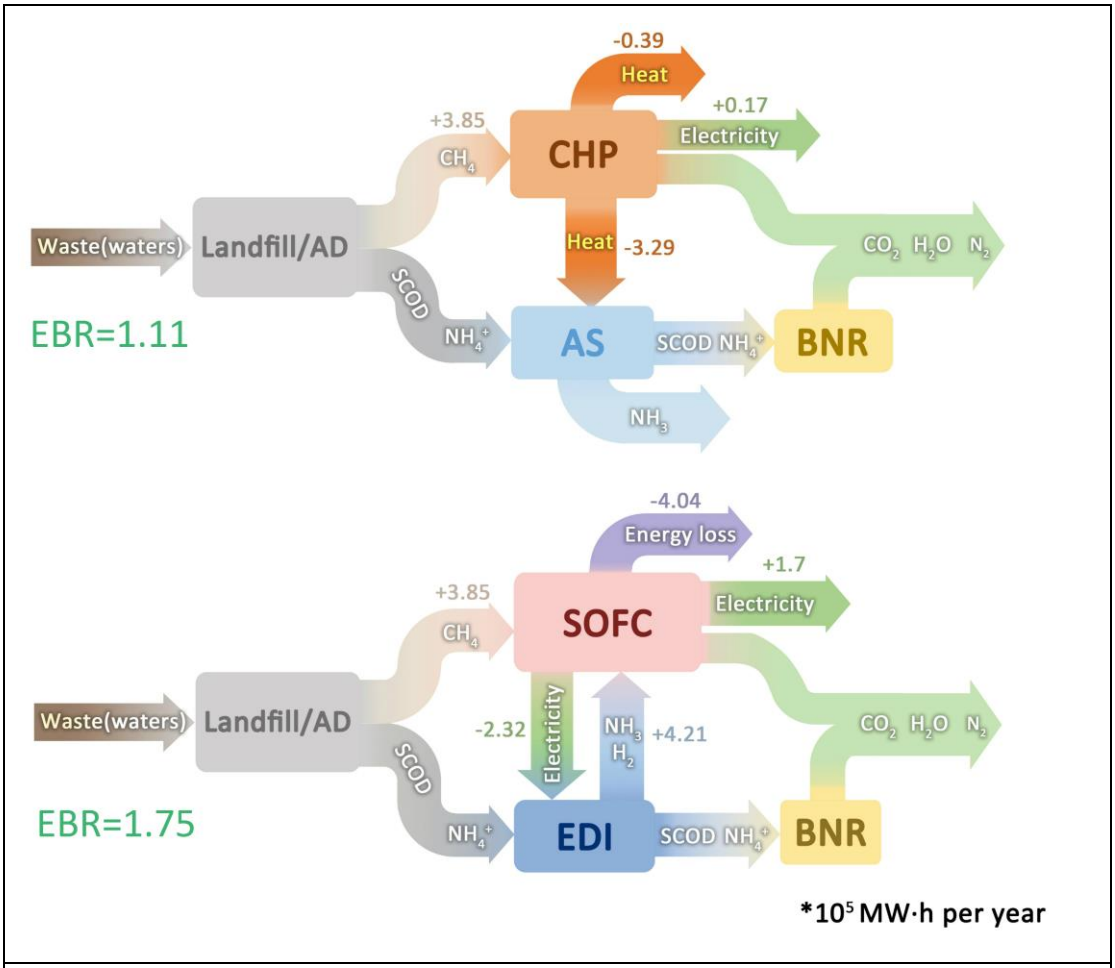

Fig. 5 Comparisons of mass and energy flow between AS–CHP and EDI–SOFC

463

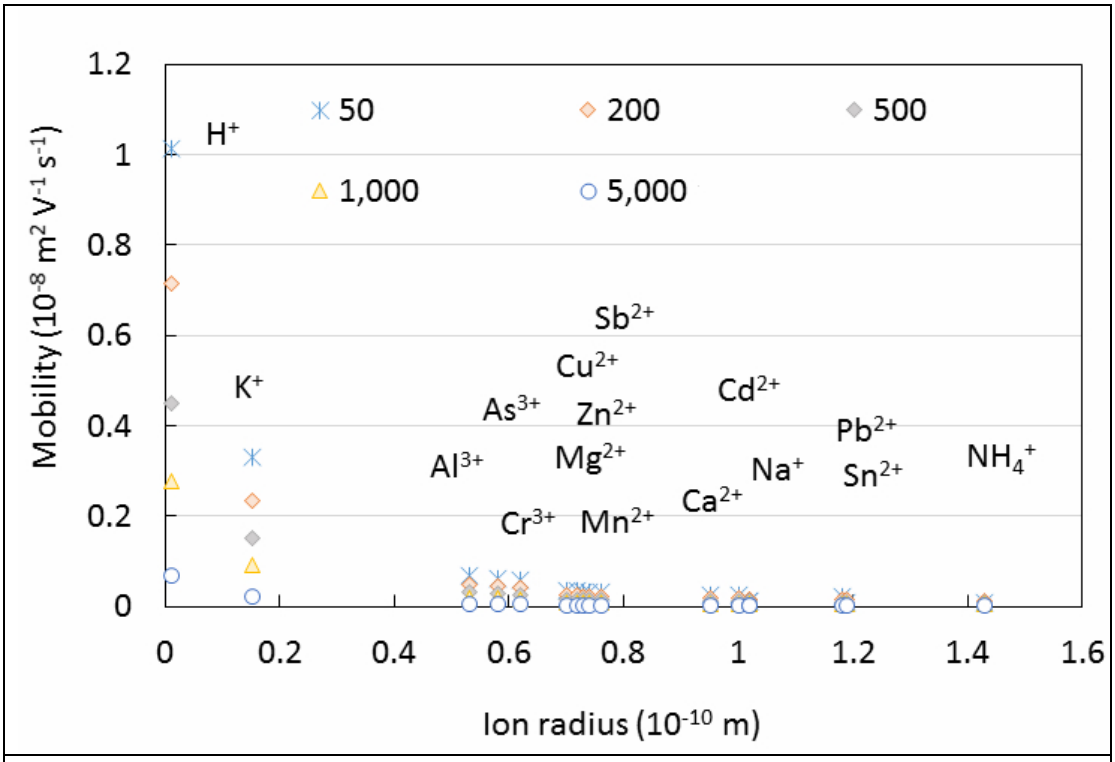

Fig. 6 Mobility of metal ions as functions of ion radii and concentration (mg L^{-1})

464

465

466

467

Notation

EDI	Electrodeionization
SOFC	Solid oxide fuel cells
COD	Chemical oxygen demand
CHP	Combined heat and power
AS	Air stripping
IED	Internal electrode distance
EBR	Energy balance ratio

468

469

470 Table 1 Energy benefits from different concentrations of ammonium wastewater through the EDI–SOFC system*

Experiment	NH_4^+-N Concentration	Deionization	Treatment Capacity	Operating Period	Energy Recovery	Energy Input	Net Energy Revenue	Energy Balance Ratio
	M	%	$m^3\ d^{-1}$	hr		$kJ\ m^{-3}\ d^{-1}$		
Batch	0.025	95	0.00024	2	45,853.1	92,584.2	-46731.1	0.50
	0.05	92	0.00024	2	70,493.6	93,649.8	-23156.3	0.75
	0.10	87	0.00024	2	87,117.7	114,604.0	-27486.3	0.76
	0.25	83	0.00024	2	134,437.9	112,441.9	21996.0	1.20
	0.50	76	0.00024	2	185,549.8	163,890.2	21659.6	1.13
Semi-continuous	0.21	98	0.00288	0.16	71,391.2	40,578.7	30,812.5	1.76

471 * The detailed calculation is available in the supporting information.

472

473

474

Table 2 Comparisons of ammonium removal/recovery processes integrated with anaerobic treatment per removal of 1 mole of NH_4^+ with 3.47 mole of biodegradable COD (a biodegradable COD /N ratio of 7.9), typical of U.S. medium strength wastewater [80, 81].

Processes	Sludge Yield	Oxygen Requirement	Energy Sources				Energy Potential*	Energy Input**	Energy Balance Ratio	Reference
			CH_4	N_2O	NH_3	H_2				
	g		mol				kJ			
Nitrification–Denitrification	26.0	52	0.85	-	-	-	753	219.2	3.43	[82]
Nitrification–Anammox***	18.3	42	1.29	-	-	-	1142	176.9	6.45	[73]
CANDO	15.8	42	1.29	0.58	-	-	1186	176.9	6.70	[83]
EDI–SOFC	13.3	-	1.80	-	0.80	1.86	2388	113.6	21.02	This study

*Estimated according to ΔH_R^0 of Eq.1 to Eq. 6.

**1.17 kWh kg^{-1}-O_2 for aeration[84], and 2.32 kWh kg^{-1}-NH_3 for recovery (this study)

*** anammox: anaerobic ammonium oxidation

480 Table 3 Ions removal from the raw landfill leachate through the semi-continuous EDI

481 reactor

Pollutants	Raw Landfill Leachate	EDI Effluent	Removal Efficiency (%)
	mg L^{-1}		
PO_4^{3-}	414	20.6	95.02
NO_2^--N	1.4	0.56	96.14
NO_3^--N	104	8.5	83.65
SO_4^{2-}	319	112.5	64.73
NH_4^+	2956.6	61.5	98.97
Ag	0.24	0.02	92.59
Al	1.53	0.69	54.52
As	0.27	0.02	91.81
Ba	0.08	0.01	90.00
Ca	25.34	2.71	89.32
Co	0.10	0.02	84.31
Cr	0.79	0.02	96.97
Cu	0.05	0.00	89.71
Fe	2.13	0.08	96.07
K	884.38	1.87	99.79
Mg	60.11	2.33	96.12
Ni	0.39	0.03	92.83
Pb	0.14	0.02	85.71
Sb	0.04	0.00	94.44
Se	0.04	0.03	20.00
Sr	0.15	0.03	77.63
Zn	1.41	0.04	97.23

482
483
484
485
486
487
488
489
490
491

REFERENCES

[1] T. Abbasi, S. Tauseef, S. Abbasi. Anaerobic digestion for global warming control and energy generation: An overview. Renew Sust Energ Rev. 16 (2012) 3228-42.

[2] D.O. Hall, G.W. Barnard, P. Moss. Biomass for energy in the developing countries: current role, potential, problems, prospects. Elsevier2013.

[3] J. Frijns, J. Hofman, M. Nederlof. The potential of (waste) water as energy carrier. Energy Conversion and Management. 65 (2013) 357-63.

[4] J. Song, W. Yang, Z. Li, Y. Higano, X.e. Wang. Discovering the energy, economic and environmental potentials of urban wastes: An input–output model for a metropolis case. Energy Conversion and Management. 114 (2016) 168-79.

[5] P. Jain, J.T. Powell, J.L. Smith, T.G. Townsend, T. Tolaymat. Life-cycle inventory and impact evaluation of mining municipal solid waste landfills. Environ Sci Technol. 48 (2014) 2920-7.

[6] M.R. Daelman, E.M. van Voorthuizen, U.G. van Dongen, E.I. Volcke, M.C. van Loosdrecht. Methane emission during municipal wastewater treatment. Water Res 46 (2012) 3657-70.

[7] O.P. Karthikeyan, C. Visvanathan. Bio-energy recovery from high-solid organic substrates by dry anaerobic bio-conversion processes: A review. Rev Environ Sci Biotechnol. 12 (2013) 257-84.

[8] M. Raboni, V. Torretta, P. Viotti, G. Urbini. Experimental plant for the physical-chemical treatment of groundwater polluted by municipal solid waste (MSW) leachate, with ammonia recovery. Rev Ambient Água. 8 (2013) 22-32.

[9] M. Lantz. The economic performance of combined heat and power from biogas produced from manure in Sweden: A comparison of different CHP technologies. Appl Energ. 98 (2012) 502-11.

[10] S. Wongchanapai, H. Iwai, M. Saito, H. Yoshida. Performance evaluation of a direct-biogas solid oxide fuel cell-micro gas turbine (SOFC-MGT) hybrid combined heat and power (CHP) system. J Power Sources. 223 (2013) 9-17.

[11] E. León, M. Martín. Optimal production of power in a combined cycle from manure based biogas. Energy Conversion and Management. 114 (2016) 89-99.

[12] A. Bogusch, R.T. Grubbs. Austin Water Utility's Hornsby Bend Biogas-to-Energy CHP Project–Commissioning and startup. J Water Pollut Control Fed 2014 (2014) 1-14.

[13] N. de Arespacochaga, C. Valderrama, C. Peregrina, A. Hornero, L. Bouchy, J. Cortina. On-site cogeneration with sewage biogas via high-temperature fuel cells: Benchmarking against other options based on industrial-scale data. Fuel Process Technol 138 (2015) 654-62.

[14] D. Wu, R. Wang. Combined cooling, heating and power: a review. Prog Energy Combust Sci. 32 (2006) 459-95.

[15] G. Venkatesh, R.A. Elmi. Economic-environmental analysis of handling biogas from sewage sludge digesters in WWTPs (wastewater treatment plants) for energy recovery: Case study of Bekkelaget WWTP in Oslo (Norway). Energy. 58 (2013) 220-35.

[16] A.L. Smith, L.B. Stadler, L. Cao, N.G. Love, L. Raskin, S.J. Skerlos. Navigating wastewater energy recovery strategies: A life cycle comparison of anaerobic membrane bioreactor and conventional treatment systems with anaerobic digestion. Environ Sci Technol. 48 (2014) 5972-81.

[17] P. McKendry. Energy production from biomass (Part 2): Conversion technologies. Bioresour Technol 83 (2002) 47-54.

[18] L. Lin, S. Yuan, J. Chen, Z. Xu, X. Lu. Removal of ammonia nitrogen in wastewater by microwave radiation. J Hazard Mater 161 (2009) 1063-8.

[19] K. Cheung, L. Chu, M. Wong. Ammonia stripping as a pretreatment for landfill leachate. Water Air Soil Poll. 94 (1997) 209-21.
[20] A. Serna-Maza, S. Heaven, C.J. Banks. Biogas stripping of ammonia from fresh digestate from a food waste digester. Bioresour Technol 190 (2015) 66-75.
[21] S. Hussain, H.A. Aziz, M.H. Isa, M.N. Adlan, F.A.H. Asaari. Physico-chemical method for ammonia removal from synthetic wastewater using limestone and GAC in batch and column studies. Bioresour Technol 98 (2007) 874-80.
[22] J. Desloover, A. Abate Woldeyohannis, W. Verstraete, N. Boon, K. Rabaey. Electrochemical resource recovery from digestate to prevent ammonia toxicity during anaerobic digestion. Environ Sci Technol. 46 (2012) 12209-16.
[23] Y.D. Scherson, G.F. Wells, S.-G. Woo, J. Lee, J. Park, B.J. Cantwell, et al. Nitrogen removal with energy recovery through N 2 O decomposition. Energ Environ Sci. 6 (2013) 241-8.
[24] A. Klerke, Christensen, C. H., Nørskov, J. K., & Vegge, T. Ammonia for hydrogen storage: Challenges and opportunities. J Mater Chem (2008) 18(20), 2304-10.
[25] F. Schüth, R. Palkovits, R. Schlögl, D.S. Su. Ammonia as a possible element in an energy infrastructure: catalysts for ammonia decomposition. Energ Environ Sci. 5 (2012) 6278-89.
[26] L. Green. An ammonia energy vector for the hydrogen economy. Int J Hydrogen Energy. 7 (1982) 355-9.
[27] P.W. Atkins, J. de Paula. Physikalische chemie. John Wiley & Sons2013.
[28] R. Lan, S. Tao, J.T. Irvine. A direct urea fuel cell: Power from fertiliser and waste. Energ Environ Sci. 3 (2010) 438-41.
[29] B. Schartel, U. Braun, U. Schwarz, S. Reinemann. Fire retardancy of polypropylene/flax blends. Polymer. 44 (2003) 6241-50.
[30] J.H. Ahn, S. Kim, H. Park, B. Rahm, K. Pagilla, K. Chandran. N2O emissions from activated sludge processes, 2008− 2009: Results of a national monitoring survey in the United States. Environ Sci Technol. 44 (2010) 4505-11.
[31] W. Wang, R. Ran, C. Su, Y. Guo, D. Farrusseng, Z. Shao. Ammonia-mediated suppression of coke formation in direct-methane solid oxide fuel cells with nickel-based anodes. J Power Sources. 240 (2013) 232-40.
[32] F. Siavashi, M. Saidi, M.R. Rahimpour. Purge gas recovery of ammonia synthesis plant by integrated configuration of catalytic hydrogen-permselective membrane reactor and solid oxide fuel cell as a novel technology. J Power Sources. 267 (2014) 104-16.
[33] H. Tsukuda, A. Notomi, N. Histatome. Application of plasma spraying to tubular-type solid oxide fuel cells production. J Therm Spray Technol. 9 (2000) 364-8.
[34] B. Tjaden, M. Gandiglio, A. Lanzini, M. Santarelli, M. Jarvinen. Small-scale biogas-SOFC plant: technical analysis and assessment of different fuel reforming options. Energy Fuels. 28 (2014) 4216-32.
[35] A. Lanzini, P. Leone. Experimental investigation of direct internal reforming of biogas in solid oxide fuel cells. Int J Hydrogen Energy. 35 (2010) 2463-76.
[36] V. Chiodo, A. Galvagno, A. Lanzini, D. Papurello, F. Urbani, M. Santarelli, et al. Biogas reforming process investigation for SOFC application. Energy Convers Manage. 98 (2015) 252-8.
[37] J. Ma, C. Jiang, P.A. Connor, M. Cassidy, J.T. Irvine. Highly efficient, coking-resistant SOFCs for energy conversion using biogas fuels. Journal of Materials Chemistry A. 3 (2015) 19068-76.
[38] A.B. Stambouli, E. Traversa. Solid oxide fuel cells (SOFCs): A review of an environmentally clean and efficient source of energy. Renew Sust Energ Rev. 6 (2002) 433-55.

[39] Y. Lin, R. Ran, Y. Guo, W. Zhou, R. Cai, J. Wang, et al. Proton-conducting fuel cells operating on hydrogen, ammonia and hydrazine at intermediate temperatures. Int J Hydrogen Energy. 35 (2010) 2637-42.
[40] E. Idelovitch, M. Michail. Nitrogen removal by free ammonia stripping from high pH ponds. J Water Pollut Control Fed (1981) 1391-401.
[41] L. Zhang, Y.-W. Lee, D. Jahng. Ammonia stripping for enhanced biomethanization of piggery wastewater. J Hazard Mater 199 (2012) 36-42.
[42] H.U. Cho, S.K. Park, J.H. Ha, J.M. Park. An innovative sewage sludge reduction by using a combined mesophilic anaerobic and thermophilic aerobic process with thermal-alkaline treatment and sludge recirculation. J Environ Manage 129 (2013) 274-82.
[43] M. Parmar, L.S. Thakur. Heavy metal Cu, Ni and Zn: Toxicity, health hazards and their removal techniques by low cost adsorbents: A short overview. Int J Plant Anim Environ Sci. (2013) 3(), 143-57.
[44] S. Srivastava, P. Goyal. Novel biomaterials: Decontamination of toxic metals from wastewater. Springer Science & Business Media.2010.
[45] M. Mondor, L. Masse, D. Ippersiel, F. Lamarche, D.I. Masse. Use of electrodialysis and reverse osmosis for the recovery and concentration of ammonia from swine manure. Bioresour Technol 99 (2008) 7363-8.
[46] M. Mehanna, P.D. Kiely, D.F. Call, B.E. Logan. Microbial electrodialysis cell for simultaneous water desalination and hydrogen gas production. Environ Sci Technol. 44 (2010) 9578-83.
[47] Y.-M. Kim, P. Kim-Lohsoontorn, S.-W. Baek, J. Bae. Electrochemical performance of unsintered Ba 0.5 Sr 0.5 Co 0.8 Fe 0.2 O 3− δ, La 0.6 Sr 0.4 Co 0.8 Fe 0.2 O 3− δ, and La 0.8 Sr 0.2 MnO 3− δ cathodes for metal-supported solid oxide fuel cells. International Journal of Hydrogen Energy. 36 (2011) 3138-46.
[48] D. Heidari, S. Javadpour, S.H. Chan. Optimization of BSCF-SDC composite air electrode for intermediate temperature solid oxide electrolyzer cell. Energy Conversion and Management. 136 (2017) 78-84.
[49] W. Zhou, L. Ge, Z.-G. Chen, F. Liang, H.-Y. Xu, J. Motuzas, et al. Amorphous iron oxide decorated 3D heterostructured electrode for highly efficient oxygen reduction. Chemistry of Materials. 23 (2011) 4193-8.
[50] F. Dong, Y. Chen, D. Chen, Z. Shao. Surprisingly high activity for oxygen reduction reaction of selected oxides lacking long oxygen-ion diffusion paths at intermediate temperatures: A case study of cobalt-free BaFeO3-δ. ACS Appl Mater Interfaces. 6 (2014) 11180-9.
[51] E.W. Rice, R.B. Baird, A.D. Eaton, L. Clesceri. Standard methods for the examination of water and wastewater. American Public Health Association, Washington, DC. (2012).
[52] S. Ramió-Pujol, R. Ganigué, L. Bañeras, J. Colprim. Incubation at 25 Celsius prevents acid crash and enhances alcohol production in Clostridium carboxidivorans P7. Bioresource Technol. 192 (2015) 296-303.
[53] B. Dai, M. Cao, G. Fang, B. Liu, X. Dong, M. Pan, et al. Schiff base-chitosan grafted multiwalled carbon nanotubes as a novel solid-phase extraction adsorbent for determination of heavy metal by ICP-MS. J Hazard Mat. 219 (2012) 103-10.
[54] D. Ippersiel, M. Mondor, F. Lamarche, F. Tremblay, J. Dubreuil, L. Masse. Nitrogen potential recovery and concentration of ammonia from swine manure using electrodialysis coupled with air stripping. J Environ Manage. 95 (2012) S165-S9.
[55] D.J. Griffiths, R. College. Introduction to electrodynamics. Prentice Hall Upper Saddle River, NJ1999.
[56] X. Chen, Y. Tang, S. Wang, Y. Song, F. Tang, X. Wu. Field-amplified sample injection in capillary

electrophoresis with amperometric detection for the ultratrace analysis of diastereomeric ephedrine alkaloids. Electrophoresis. 36 (2015) 1953-61.
[57] P. Biesheuvel, R. Zhao, S. Porada, A. Van der Wal. Theory of membrane capacitive deionization including the effect of the electrode pore space. J Colloid Interface Sci 360 (2011) 239-48.
[58] P. Biesheuvel, A. Van der Wal. Membrane capacitive deionization. J Memb Sci. 346 (2010) 256-62.
[59] A. Salis, B.W. Ninham. Models and mechanisms of Hofmeister effects in electrolyte solutions, and colloid and protein systems revisited. Chem Soc Rev. 43 (2014) 7358-77.
[60] E. Simons, E. Cairns, D. Surd. The performance of direct ammonia fuel cells. J Electrochem Soc 116 (1969) 556-61.
[61] Q. Ma, J. Ma, S. Zhou, R. Yan, J. Gao, G. Meng. A high-performance ammonia-fueled SOFC based on a YSZ thin-film electrolyte. J Power Sources. 164 (2007) 86-9.
[62] G. Meng, C. Jiang, J. Ma, Q. Ma, X. Liu. Comparative study on the performance of a SDC-based SOFC fueled by ammonia and hydrogen. J Power Sources. 173 (2007) 189-93.
[63] D. Cheddie. Ammonia as a hydrogen source for fuel cells: A review. system. 250 (2012) 400.
[64] S. Hajimolana, M. Hussain, W. Wan Daud. Comparativestudy on the performance of a tubular solid oxide fuel cell fuelled by ammonia and hydrogen. Chemeca 2011: Engineering a Better World: Sydney Hilton Hotel, NSW, Australia, 18-21 September 2011. (2011) 2021.
[65] G.N. Krishnan, P. Jayaweera, J. Perez, M. Hornbostel, J.R. Albritton, R.P. Gupta. Effect of coal contaminants on solid oxide fuel system performance and service life. Sri International2007.
[66] N.S. Spinner, J.A. Vega, W.E. Mustain. Recent progress in the electrochemical conversion and utilization of CO2. Catal Sci Technol. 2 (2012) 19-28.
[67] I. Dincer, C.O. Colpan, O. Kizilkan, M.A. Ezan. Progress in clean energy. Springer2015.
[68] B. Suddhasatwa. Recent trends in fuel cell science and technology. New York, USA, Springer press2007.
[69] M. Kuhn, T.W. Napporn. Single-chamber solid oxide fuel cell technology—From its origins to today's state of the art. Energies. 3 (2010) 57-134.
[70] D. Singh, E. Hernández-Pacheco, P.N. Hutton, N. Patel, M.D. Mann. Carbon deposition in an SOFC fueled by tar-laden biomass gas: A thermodynamic analysis. J Power Sources. 142 (2005) 194-9.
[71] Y. Yi, A.D. Rao, J. Brouwer, G.S. Samuelsen. Analysis and optimization of a solid oxide fuel cell and intercooled gas turbine (SOFC–ICGT) hybrid cycle. J Power Sources. 132 (2004) 77-85.
[72] B. Wett. Development and implementation of a robust deammonification process. Water Sci Technol 56 (2007) 81-8.
[73] v. Dongen, L.G.J.M., M. Jetten, M.v. Loosdrecht, M. C.M. The Combined Sharon/Anammox Process-A Sustainable Method for N-removal from Sludge Water2007.
[74] S.G. Sommer, M.L. Christensen, T. Schmidt, L.S. Jensen. Animal manure recycling: treatment and management. John Wiley & Sons2013.
[75] K. Foo, B. Hameed. An overview of landfill leachate treatment via activated carbon adsorption process. J Hazard Mat. 171 (2009) 54-60.
[76] T. Sokalski, P. Lingenfelter, A. Lewenstam. Numerical solution of the coupled Nernst-Planck and Poisson equations for liquid junction and ion selective membrane potentials. J Phys Chem B. 107 (2003) 2443-52.
[77] F. Harnisch, R. Warmbier, R. Schneider, U. Schröder. Modeling the ion transfer and polarization of ion exchange membranes in bioelectrochemical systems. Bioelectrochemistry. 75 (2009) 136-41.
[78] M.R. Anouti, J. Jacquemin, P. Porion. Transport properties investigation of aqueous protic ionic

667 liquid solutions through conductivity, viscosity, and NMR self-diffusion measurements. J Phys Chem B.
668 116 (2012) 4228-38.
669 [79] M.Á. de la Rubia, M. Walker, S. Heaven, C.J. Banks, R. Borja. Preliminary trials of in situ ammonia
670 stripping from source segregated domestic food waste digestate using biogas: Effect of temperature and
671 flow rate. Bioresource Technol. 101 (2010) 9486-92.
672 [80] M. Safoniuk. Wastewater engineering: Treatment and reuse. Chem Eng J 111 (2004) 10-2.
673 [81] M. Henze. Biological wastewater treatment: Principles, modelling and design. IWA publishing2008.
674 [82] Q. Yang, Y. Peng, X. Liu, W. Zeng, T. Mino, H. Satoh. Nitrogen removal via nitrite from municipal
675 wastewater at low temperatures using real-time control to optimize nitrifying communities. Environ Sci
676 Technol. 41 (2007) 8159-64.
677 [83] J. Kim, K. Kim, H. Ye, E. Lee, C. Shin, P.L. McCarty, et al. Anaerobic fluidized bed membrane bioreactor
678 for wastewater treatment. Environ Sci Technol. 45 (2010) 576-81.
679 [84] A. Fenu, J. Roels, T. Wambecq, K. De Gussem, C. Thoeye, G. De Gueldre, et al. Energy audit of a full
680 scale MBR system. Desalination. 262 (2010) 121-8.
681